Mathematical Models of Skin Penetration

Michael Heisig, Arne Nägel, Gabriel Wittum
Goethe-Center for Scientific Computing
Goethe-Universität Frankfurt

9th December 2016
IMG Bruchsal

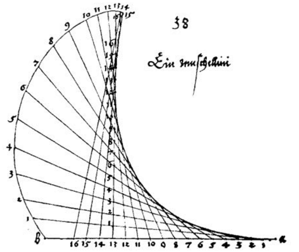

Skin as a Barrier

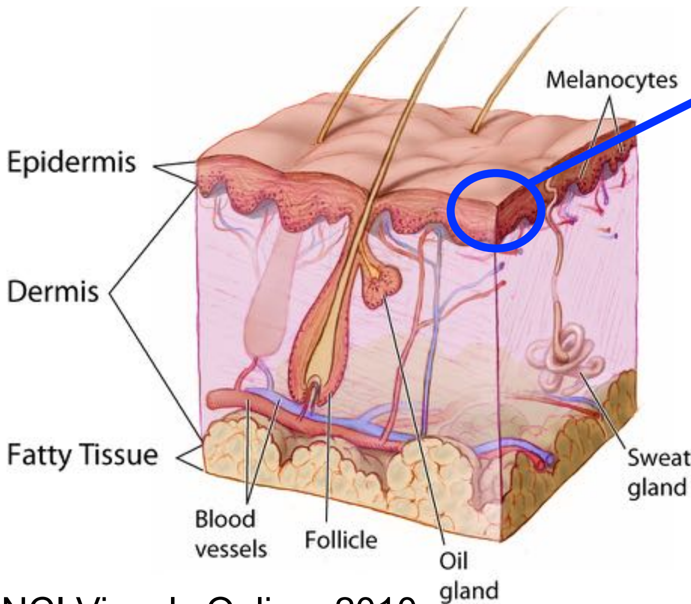

NCI Visuals Online, 2010

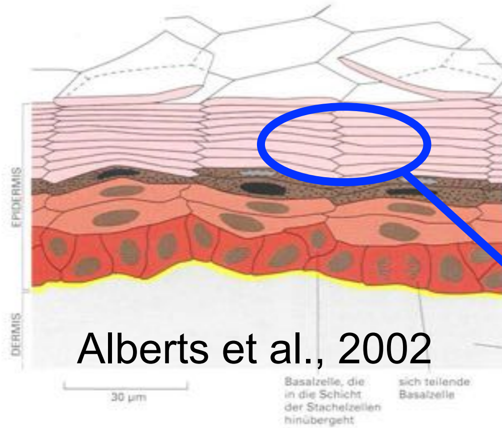

Alberts et al., 2002

Stratum Corneum
Stratum Granulosum
Stratum Spinosum
Stratum Basale

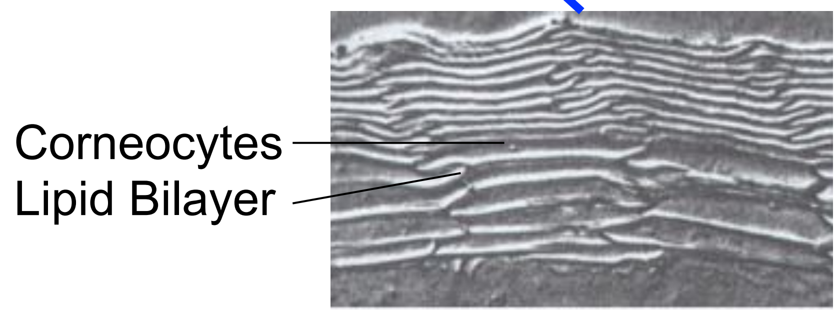

Menton and Eisen, 1971

Key functions:

- Protection from environment
- Preventing dehydration
- Anti-microbial activity
- Thermal insulation
- Shock absorption

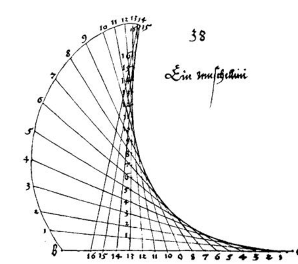

Why skin?

- Detailled knowledge about morphology available, e.g.

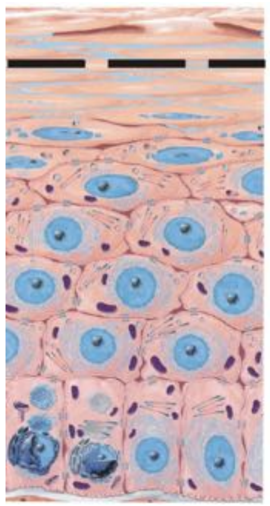

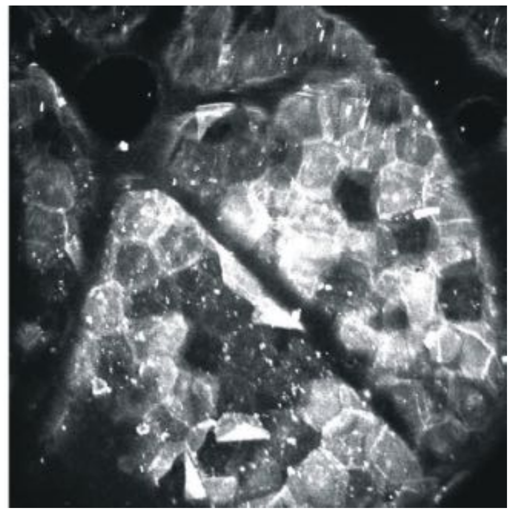

Movie courtesy of
Roger Wepf, ETH Zürich

Electron Microscopy ETH Zurich

http://www.emez.ethz.ch
http://www.cubicice.de

- Epidermis ~ highly heterogeneous, stratified epithelial layer
- State-of-the-art models primarily focus on penetration
- Yet, Differentiation and homeostatis unclear (signalling pathway, cell-cell interactions, ...)

Modeling Skin Permeability

A) Steady-state (QSPR) models

$$J_{max} = k_p\, c_{sat} = D/h * c_{sat} \quad \text{or} \quad k_p = (DK)/h$$

B) Compartmental models

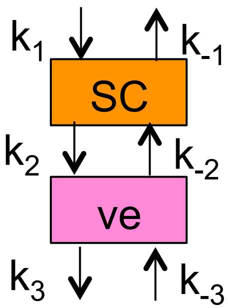

$$V_{SC}\frac{d\langle C_{SC}\rangle}{dt} = k_1 C_v - k_{-1}\langle C_{SC}\rangle - k_2\langle C_{SC}\rangle + k_{-2}\langle C_{ve}\rangle$$

$$V_{ve}\frac{d\langle C_{ve}\rangle}{dt} = k_2\langle C_{SC}\rangle - k_{-2}\langle C_{ve}\rangle - k_3\langle C_{ve}\rangle + k_{-3} C_b$$

C) Diffusion models

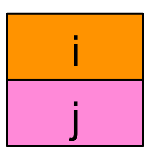

$$\frac{\partial c_i}{\partial t} + \frac{\partial}{\partial x}[-D_i \frac{\partial c_i}{\partial x}] = 0, \text{ and } c_i = K_{i/j} c_j$$

(Further reading: Mitragotri et al, 2011; various in ADDR 65, 2013;…)

Modeling Skin Permeability (2)

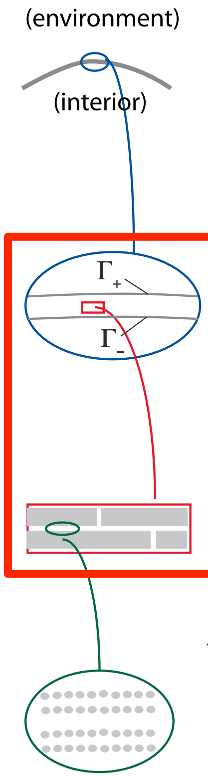

Level of detail (low → high)	Type of model	Time	Space	Comp. Complexity (low → high)
Membrane	A) Steady-state (QSPR)	✗	✗	low
	B) Compartmental models (PKPD, ODE)	✓	✗	
Cell ensemble	C1) Macroscopic Models (PDE)	✓	✓ (often 1D)	
Cellular Resolution	C2) Microscopic Models (PDE)	✓	✓ (2D, 3D)	
Molecular Resolution	*D) Molecular Dynamics*			high

Physiology based modeling (C1, C2)

Modeling Perspectives and Multiscale Character

Microscopic scale **Macroscopic scale**

Lipid Bilayer

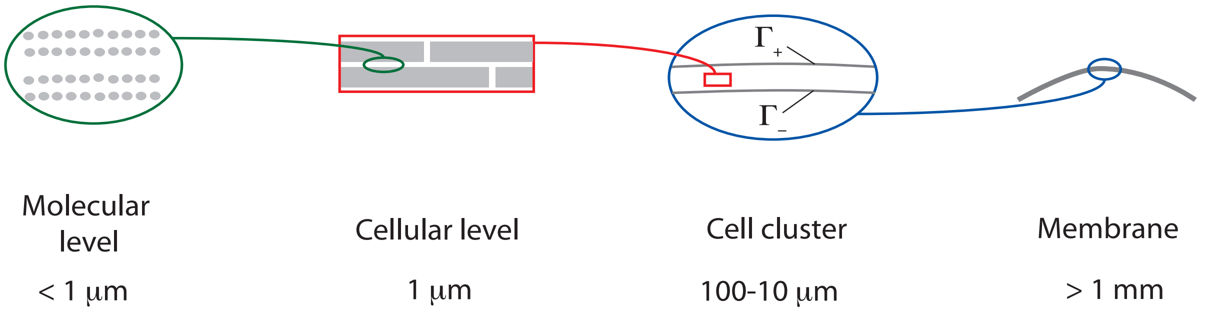

Descriptive approach (*top-down*):

- Based on observations
- Apparent (fitted) parameters
- Simple description

Mechanistic approach (*bottom-up*):

- Based on first-principles
- Function-related parameters
- Effects emerge from small to large scales

Physiology-based Modelling

① **First Principles**:

- Conservation of mass (momentum, energy, ...)

$$\frac{\partial c_i}{\partial t} + \frac{\partial}{\partial x} j_i = 0$$

② **Constitutive Relations:**

- Fick‘s law, (Hooke‘s law, ...)
- Based on observation/theroretical consideration

$$j_i := -D_i \frac{\partial c_i}{\partial x}$$

③ **Morphology:**

- Functional units are located at distinct positions, i.e., function is bound to morphology on microscopic level.

$$D_i = \dots$$

④ **Variability**

- Addressing variability between/within species

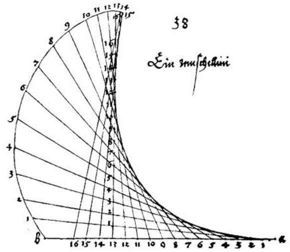

Physiology-based Modelling:
Idealized Membranes for Stratum Corneum (SC)

Cuboid

Brick-and-mortar:
Ribbon (2D), Cuboid (3D)
(Heisig et al, 1996; Wang et al., 2006; Rim et al., 2007; ...)

Elias, 1981

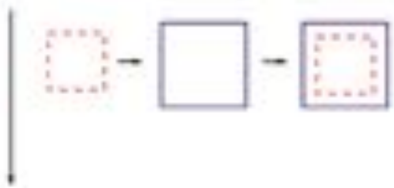

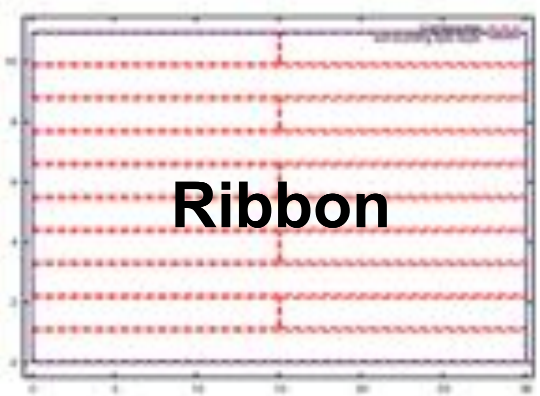

Ribbon

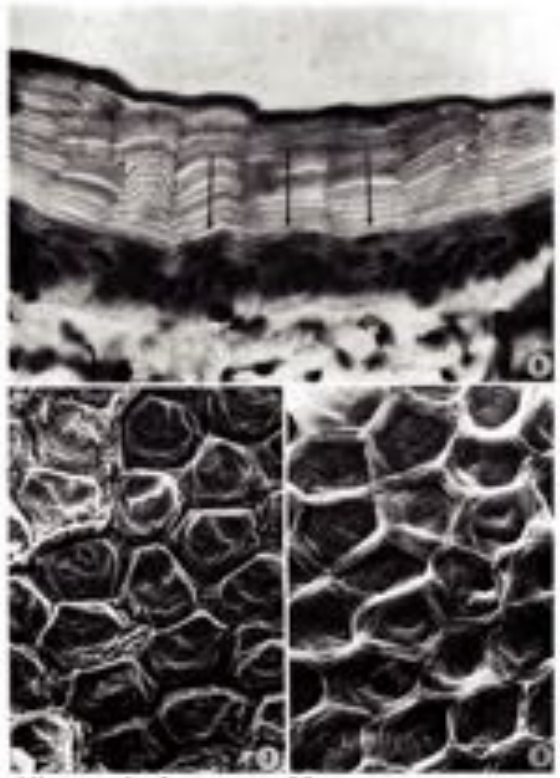

Micrograph of mouse ear SC
(D. Menton, Am J Anat, 145:1-22, 1976)

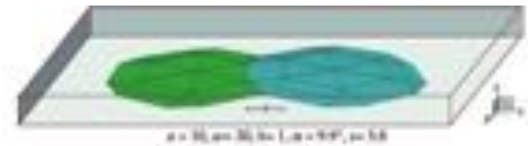

Cell-like morphology:
Tetrakaidekekahedra (3D)
(Feuchter et al., 2006)

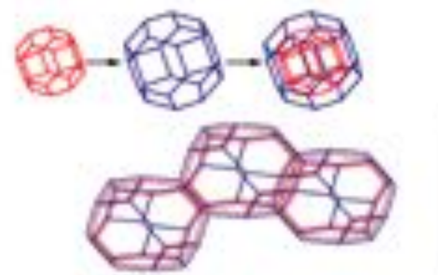

TKD

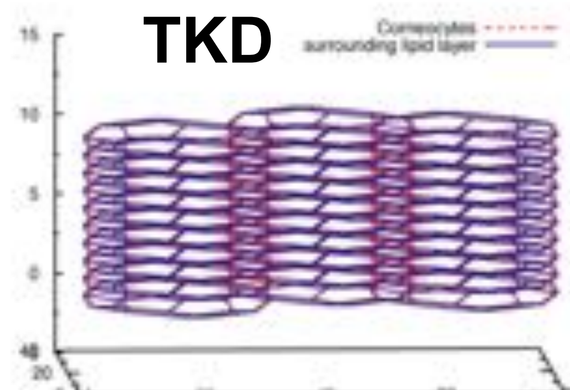

Cell Template - Tetrakaidekahedra

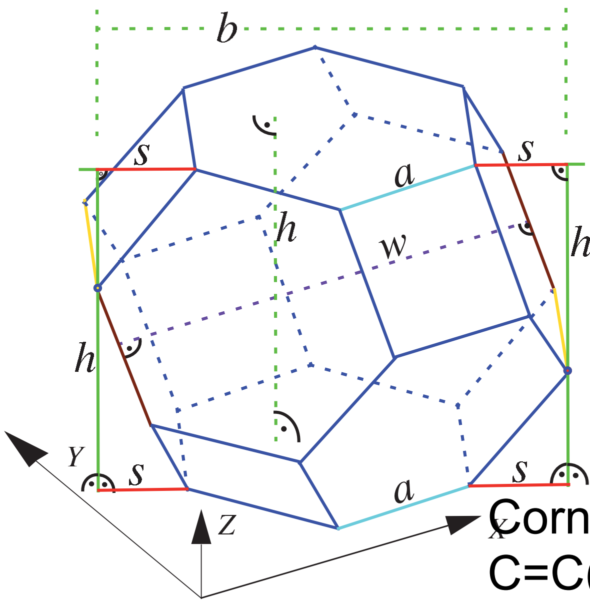

Corneocyte cell
C=C(a,h,w)

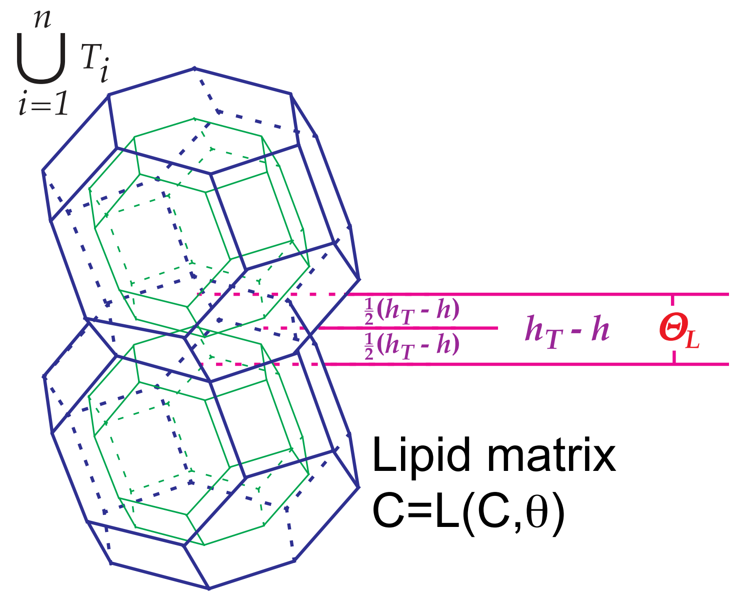

Lipid matrix
C=L(C,θ)

- TKD = Tetra-kai-deka-hedron = 4-and-10-faces (Polyhedron with 14 faces)
- Dates back to Kelvin (dense packings, foam cells): Almost optimal surface to volume ratio
- Configuration $\mathscr{C}$: Corneocyte cell C, lipid matrix L

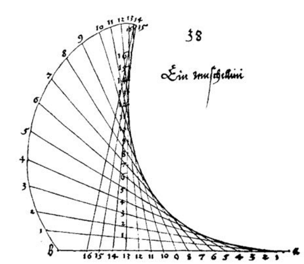

Transport equations
(e.g. Risken, 1989)

- Starting from the Fokker-Planck equation for particle density ρ

$$\frac{\partial \rho}{\partial t} + \nabla \cdot \left[-D(\vec{x}) e^{-\beta \Phi(\vec{x})} \nabla e^{\beta \Phi(\vec{x})} \rho \right] = 0$$

  with diffusion D, drift induced by force field F.

- Simplifies, assuming that (i) drift is induced by potential Φ, and (ii) a steady-state equilibrium exist (i.e., fluctuation-dissipation-theorem holds), where $\beta = (k_B T)^{-1}$

- Introducing partition coefficient $K(\vec{x}) := e^{-\beta \Phi(\vec{x})}$ and a normalized concentration $u(\vec{x}, t) := e^{\beta \Phi(\vec{x})} \rho(\vec{x}, t)$, we obtain

$$\partial_t (K u) + \nabla \cdot \left[-\mathbb{D} K \nabla u \right] = 0$$

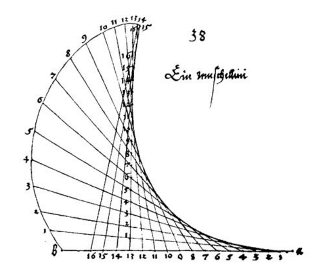

Microscopic Modelling of Stratum Corneum

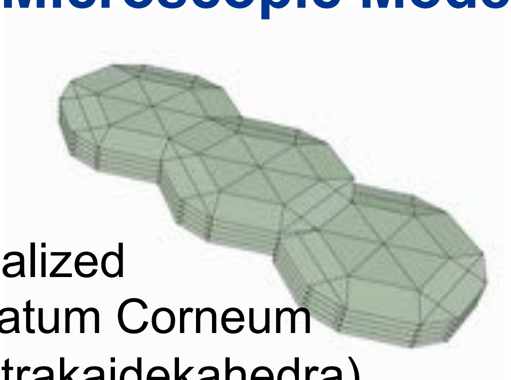

Idealized
Stratum Corneum
(Tetrakaidekahedra)

$$\partial_t(Ku) + \partial_x[-DK\partial_x u] = 0$$

Diffusion equation
(e.g. piecewise constant coefficients)

Morphology + Function = Effect

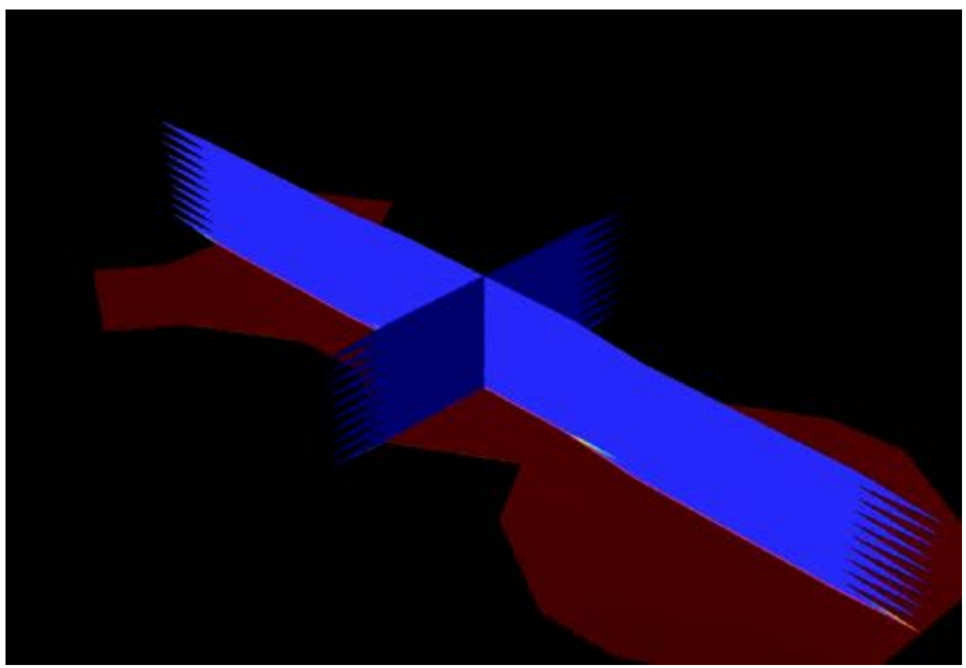

Corneocyte
sponge effect

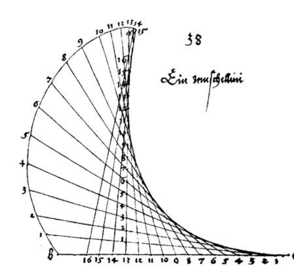

Elongated Cells lead to Anisotropic SC Diffusion

Lateral (along cells) ➔

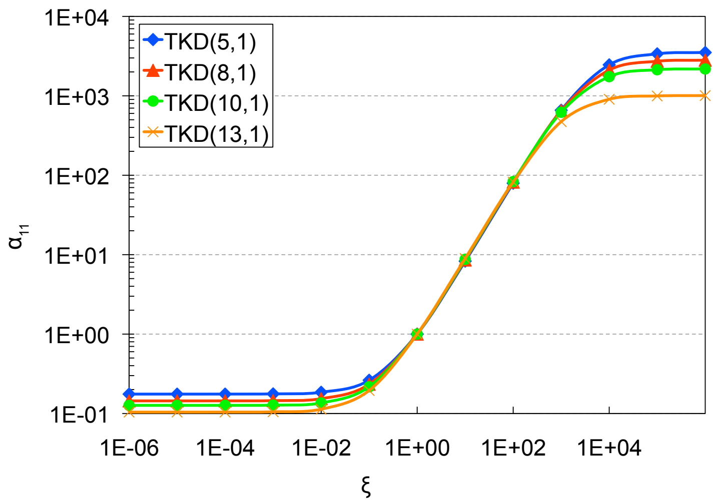

Transversal (across cells) 🡻

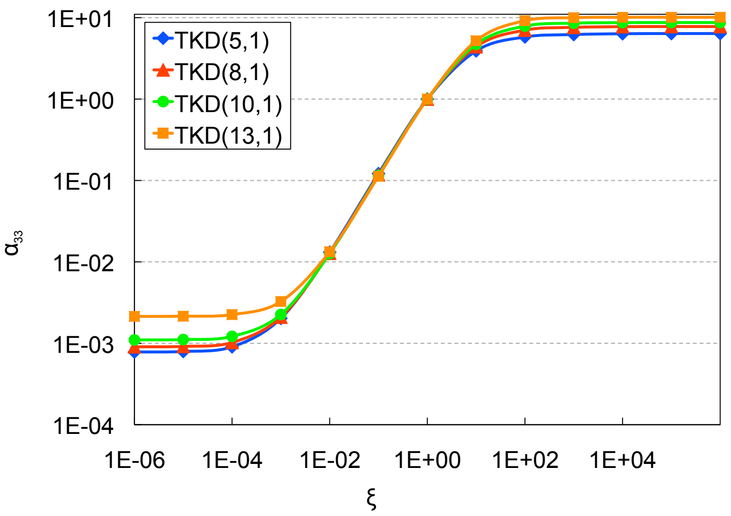

Results:

- Diagonal diffusion tensor
- Separate coefficients for lateral/transversal direction
- Dependent on effective diffusivity (sigmoidal)
- 4 parameters: D_{LIP}, D_{COR}, K_{COR}, K_{LIP}

$$\mathbb{D} = D_{lip} \begin{pmatrix} \alpha_{11}(\xi) & 0 & 0 \\ 0 & \alpha_{11}(\xi) & 0 \\ 0 & 0 & \alpha_{33}(\xi) \end{pmatrix}$$

$$\xi = \frac{D_{COR}}{D_{LIP}} K_{\mathrm{COR/LIP}}$$

Virtual Diffusion Cell
(Hansen et al., 2008; …)

2D brick-and-mortar model

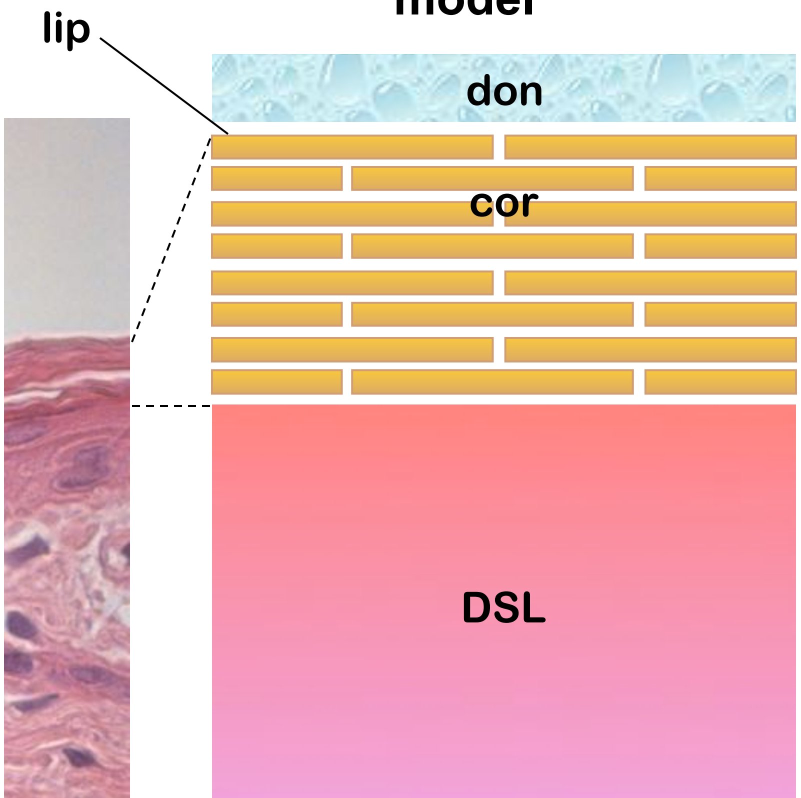

In-vitro diffusion cell

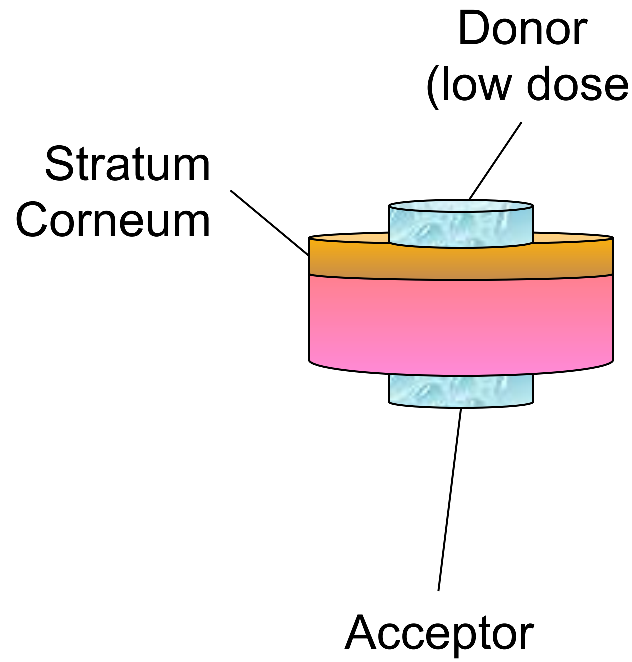

Virtual Diffusion Cell (Hansen et al., 2008; …)

2D brick-and-mortar model

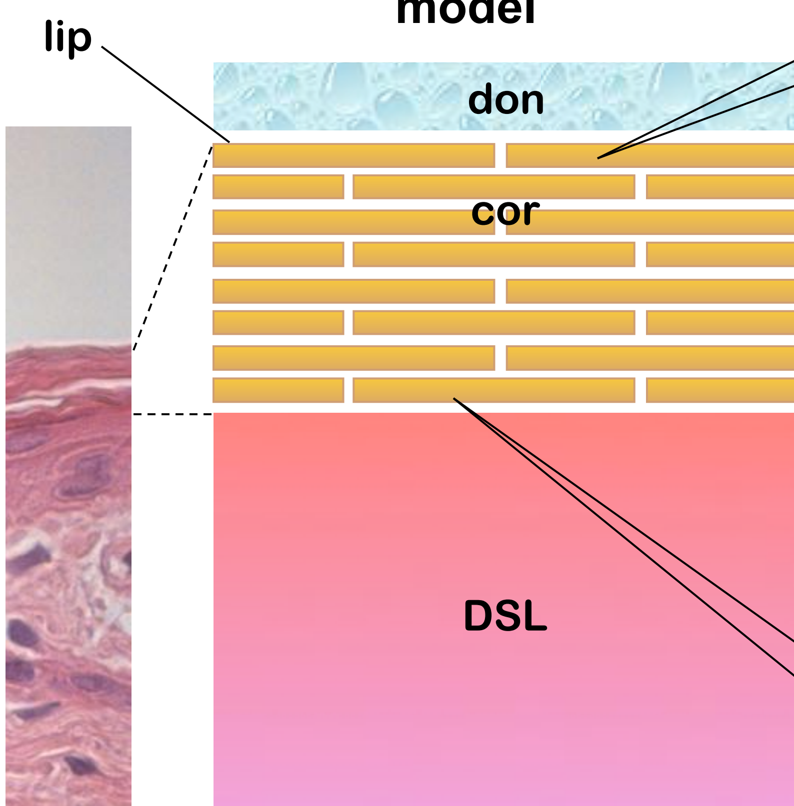

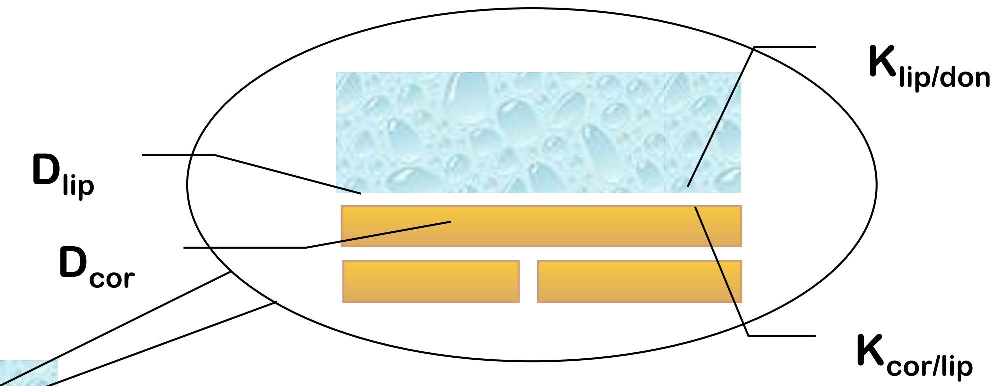

Experimental input (infinite dose)

Partitioning

- $K_{lip/don}$, $K_{SC/don}$ (equilibration)
- $K_{cor/lip}$, $K_{DSL/lip}$ (indirect)

Diffusion

- D_{lip}, D_{SC}, D_{DSL} (steady-state fluxes)
- D_{cor} (equivalent membrane)

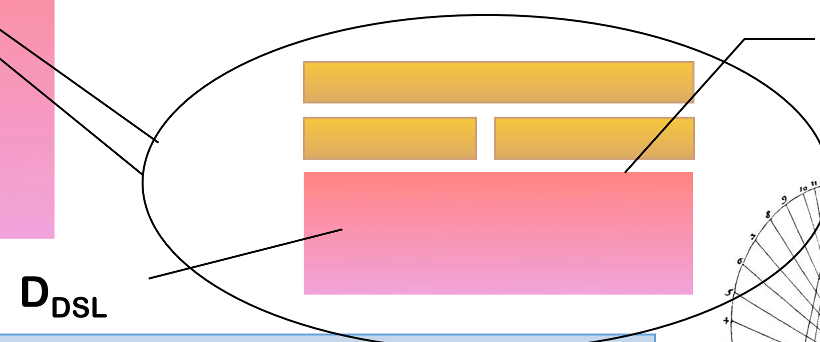

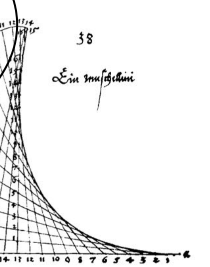

Virtual Diffusion Cell (Infinite Dose)

Parameter	Substance			
	Flufenamic acid		Caffeine	
D_{lip} (cm²/h)	1.1×10^{-4}		2.1×10^{-4}	
D_{SC} (cm²/h)	1.7×10^{-7}		1.4×10^{-7}	
D_{DSL} (cm²/h)	4.9×10^{-3}		2.3×10^{-3}	
$K_{lip/don}$	20.32		2.15	
c_{don} (mg/ml)	1.0		12.5	
	Experimental method			
	(M1)	(M2)	(M1)	(M2)
$K_{SC/don}$	16.20	5.88	4.51	4.70
$K_{cor/lip}$	0.77	0.21	2.22	2.32
$K_{DSL/lip}$	0.26	0.10	0.08	0.08
D_{cor} (cm²/h)	1.4×10^{-7}	5.1×10^{-7}	1.8×10^{-8}	1.7×10^{-8}
D^{*}_{cor} (cm²/h)	1.4×10^{-9}	5.1×10^{-9}	1.8×10^{-9}	1.7×10^{-9}

Correction of D_{COR}!

Flufenamic acid
(lipophilic, binds to keratin)

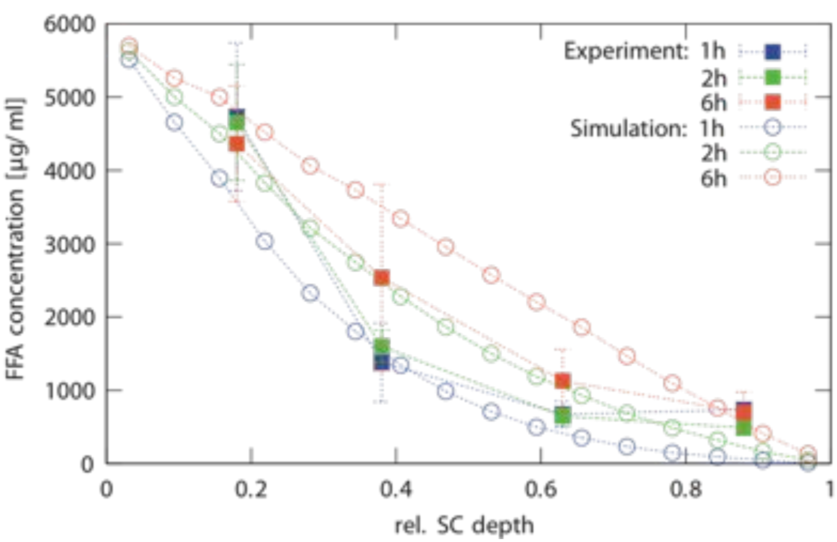

Caffeine
(hydrophilic)

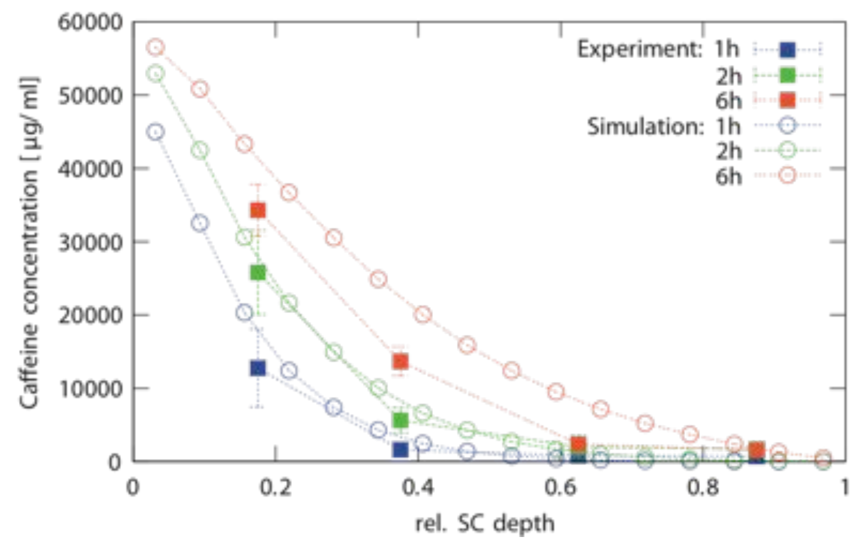

Finite dose extension: (Selzer et al., 2012; ...)

Existing models rely on trans-bilayer Correction (or: small corneocyte diffusivity)

Substance	D_{LIP}	D_{COR}	k_{trans}	D_{aq}	Reference
	(cm^2/s)	(cm^2/s)	(cm/s)	(cm^2/s)	
Ethanol	8,50E-07	1,20E-05	8,90E-05		Wang et al., 2006
Nicotinamide	9,20E-08	7,40E-06	5,90E-06		Wang et al., 2006
Testosterone	1,30E-08	3,50E-06	4,30E-07		Wang et al., 2006
Caffeine	5,83E-08	4,72E-13	---		Naegel et al., 2008
Flufenamic Acid	3,06E-08	1,42E-12	---		Naegel et al., 2008
4-Cyanophenol	3,60E-07	2,90E-11	---	9,10E-06	Lian et al., 2010

- Some parameters fitted/adjusted
- Corresponds to anisotropic diffusion in the lipids!

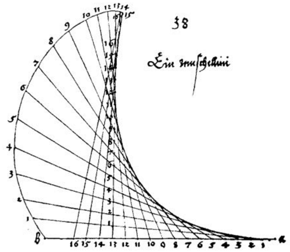

Is this relevant for Numerics?

Adaptivity reduces
Computational Complexity:

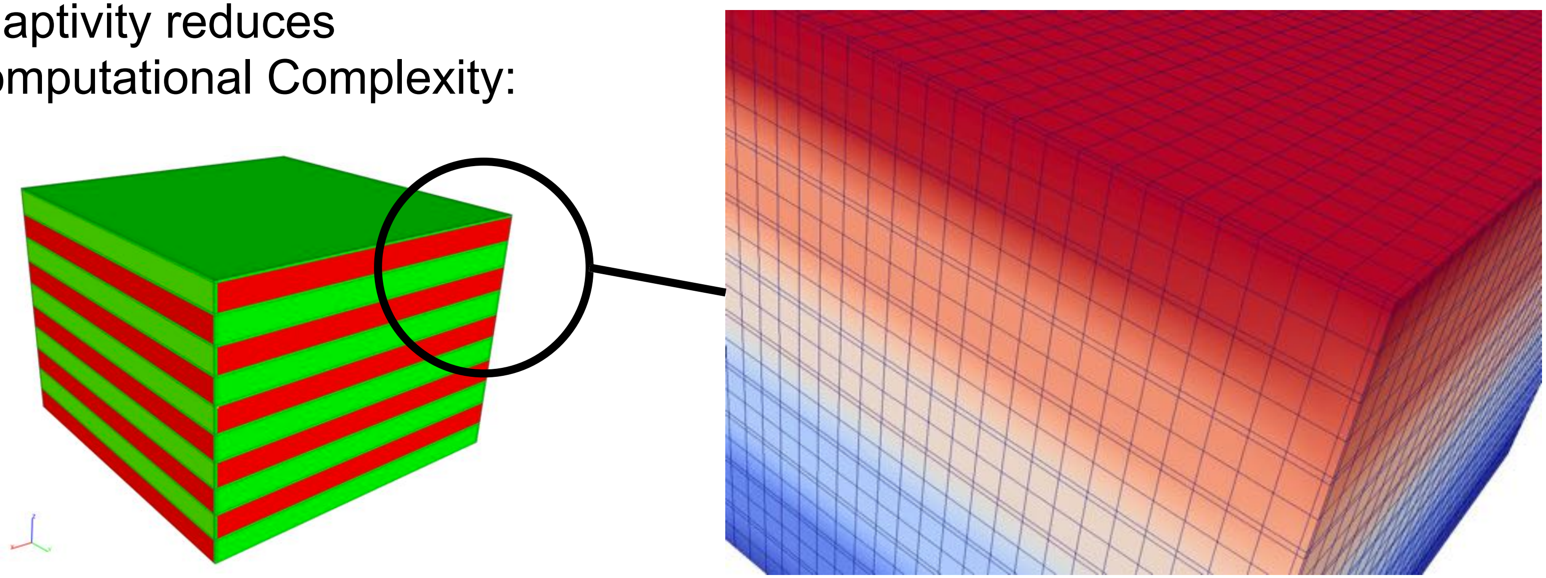

(with A. Vogel, S. Reiter, G. Wittum)

Diffusion through idealized SC w/ jumping coefficients:
$D_{LIP} = 1$, $D_{COR} = 0.001$

Singularities in the corners
➔ Refine the mesh only in this area
➔ Reduce number of degrees of freedom

Uniform vs. Adaptive refinement (steady state problem)

(with A. Vogel, S. Reiter, G. Wittum, in preparation)

Adaptive

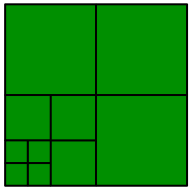

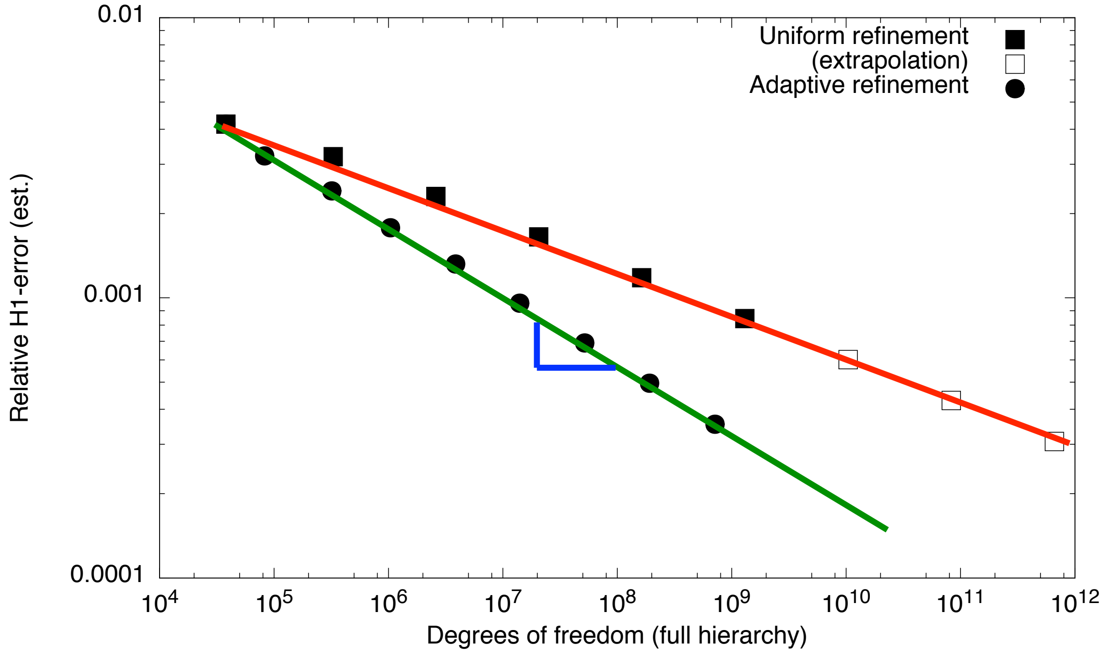

Uniform

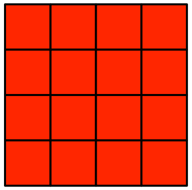

- 1K processes vs. 64 K processes
  (approx. identical wall clock time on JuQueen, JSC Jülich)

- Larger gain of accuracy per dof w/ adaptivity (still counting...)

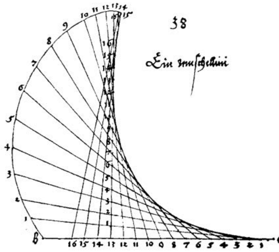

Convergence analysis

(with A. Vogel, S. Reiter,
G. Wittum, in preparation)

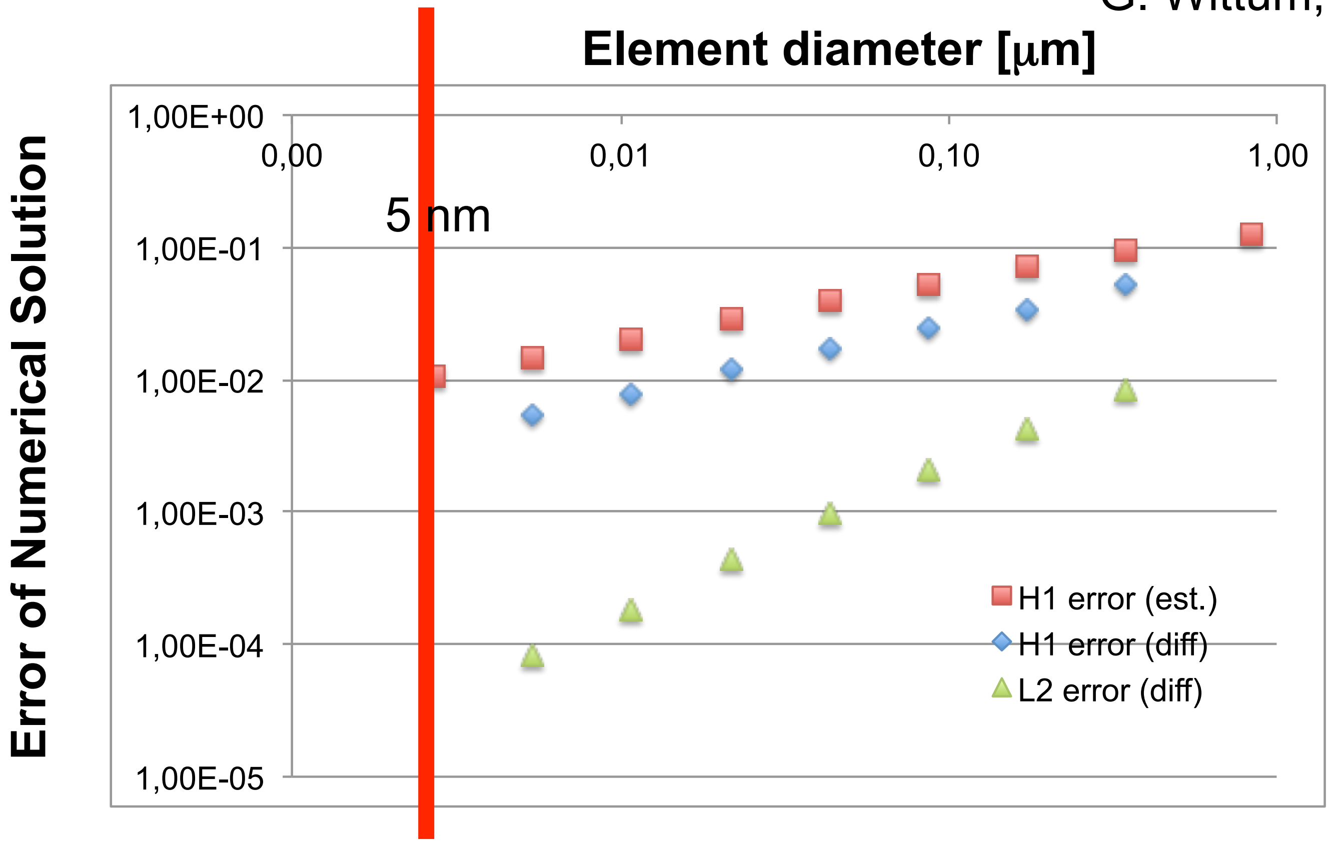

Error proportional to element diameter h:

H1-Error ~ $O(h^{1/2})$ and L2-Error ~ $O(h)$

Subscale model for SC lipids - Idea

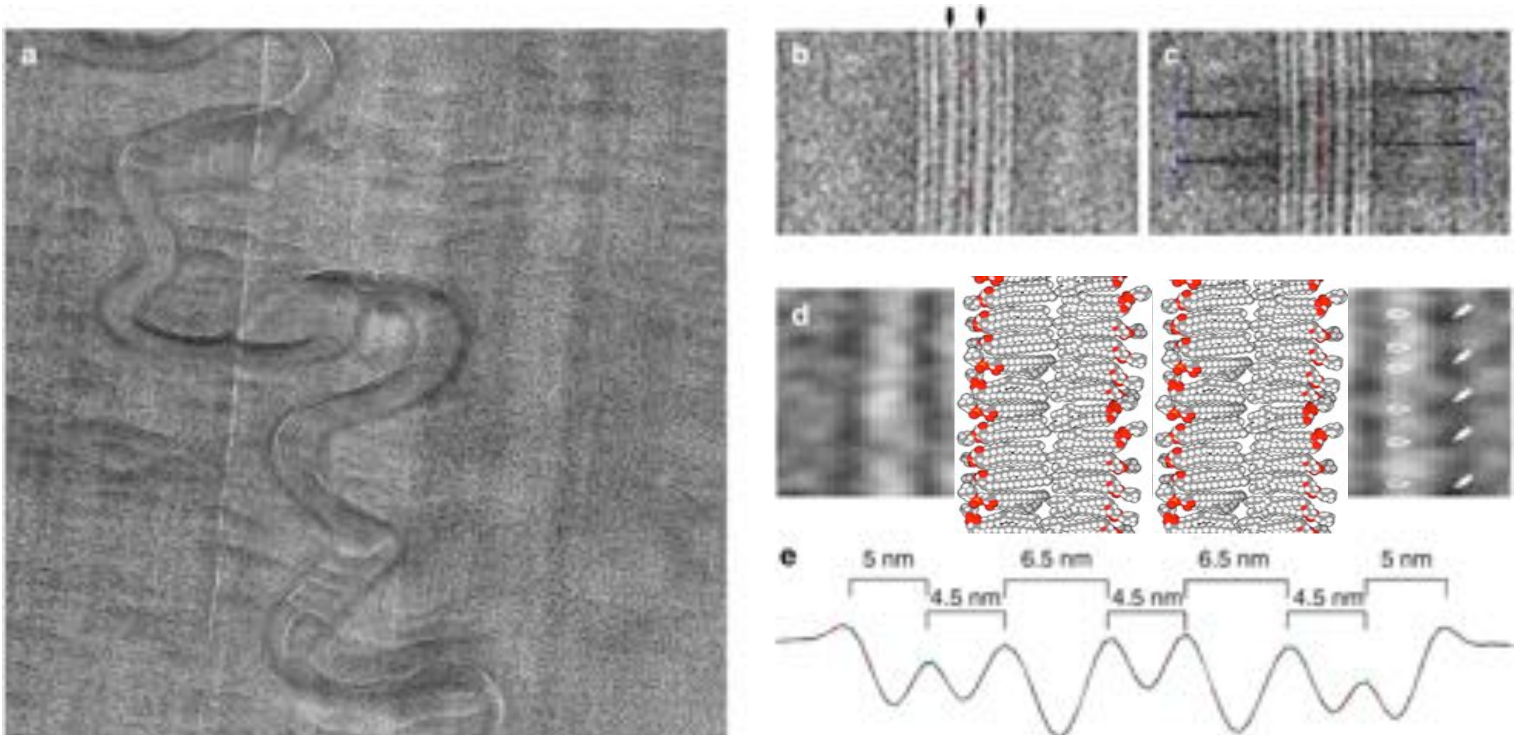

Iwai et al., JID, 2012

- The **discretization** reaches the level of **molecular resolution**
- **Fokker-Planck** equation provides **subscale model**

Subscale model for SC lipids - Homogenization

a) Lateral Diffusion ➔

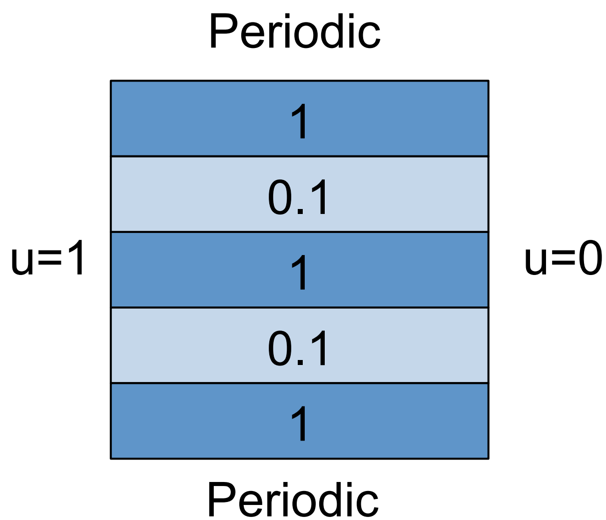

$$
\begin{aligned}
\overline{D}_{||} &= \frac{1}{L}\int_0^L D(x)\,dx \\
&= 0.6 * 1 + 0.4 * 0.1 \\
&= 0.64
\end{aligned}
$$

Anisotropic diffusion tensor **for lipids**: $\mathbb{D} = \begin{pmatrix} \overline{D}_{||} & 0 \\ 0 & \overline{D}_{\perp} \end{pmatrix}$

b) Transversal Diffusion 🡻

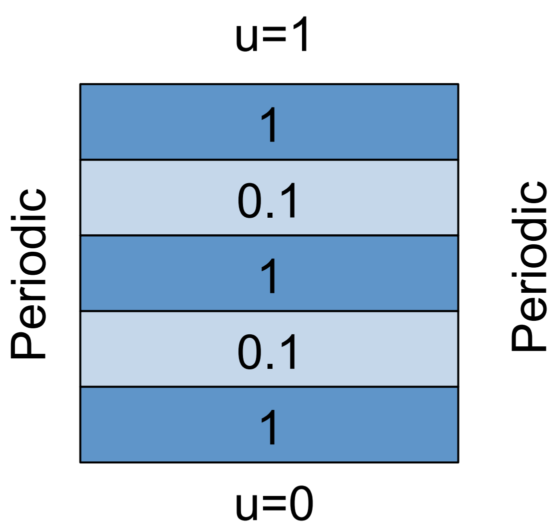

$$
\begin{aligned}
\left(\overline{D}_{\perp}\right)^{-1} &= \frac{1}{L}\int_0^L D(x)^{-1}\,dx \\
&= (0.6 * 1 + 0.4 * 10)^{-1} \\
&= (4.6)^{-1} \approx 0.21
\end{aligned}
$$

Anisotropic Lipid Diffusion

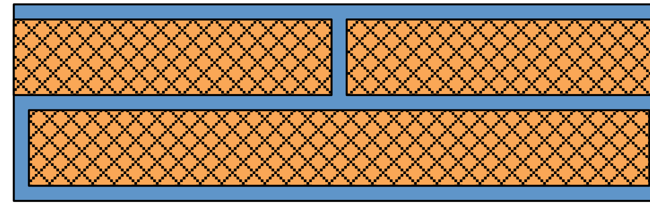

Model yields large gradients in Lipid layer:

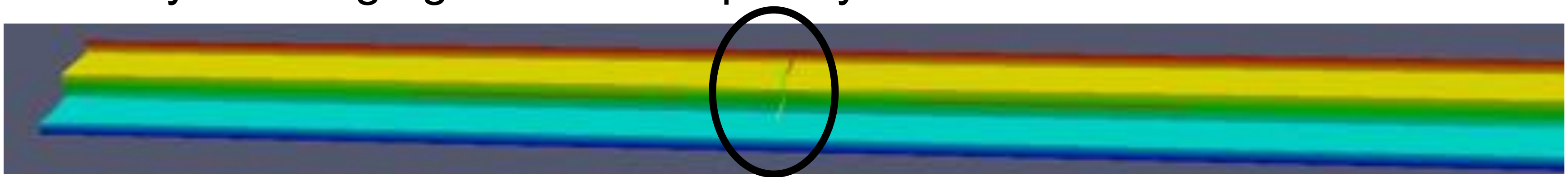

Resolved using adaptive mesh refinement:

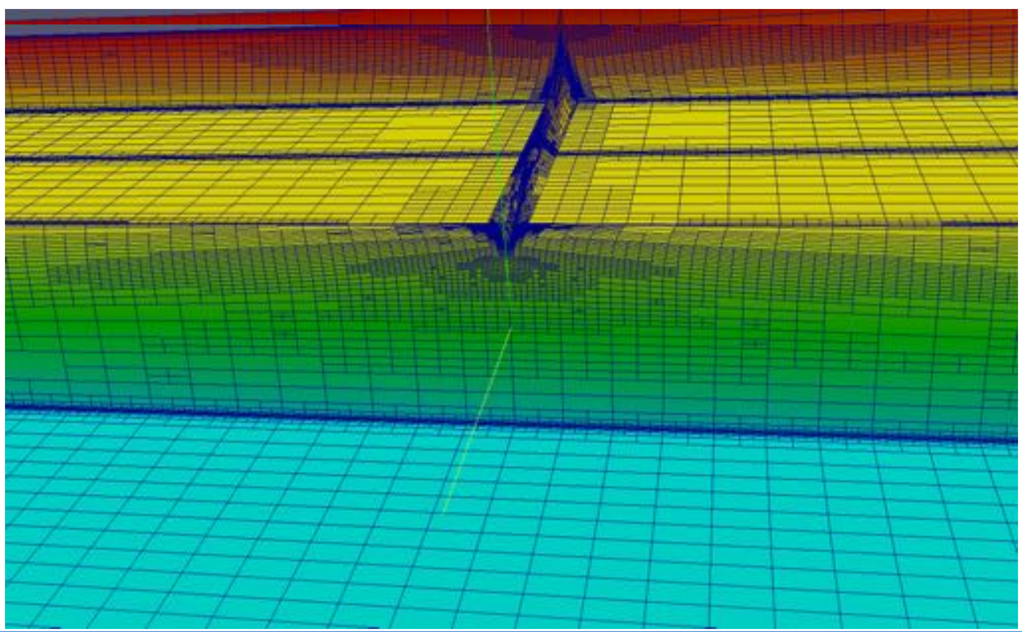

Anisotropic Lipid Diffusion as Rate Limiting Step (with J. Nitsche, unpublished)

Effective permeability of the barrier:

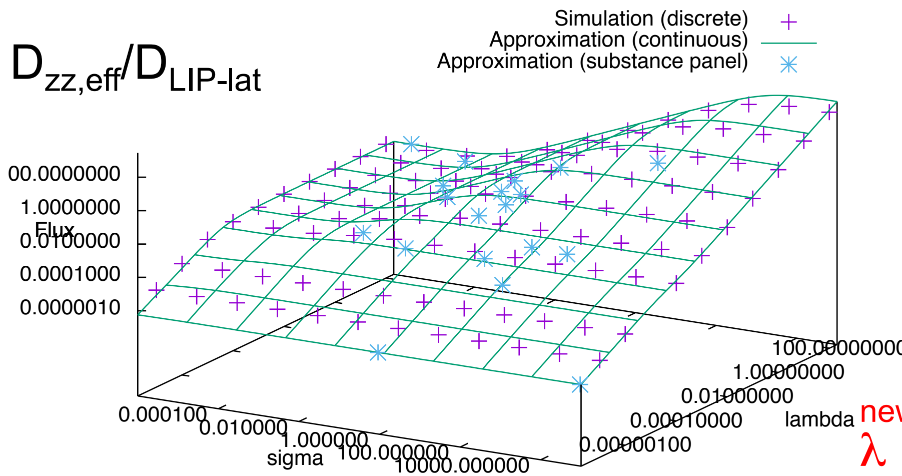

new: $\lambda = D_{LIP\text{-}trans} / D_{LIP\text{-}lat}$

$\sigma = (K_{COR} * D_{COR}) / (K_{LIP} * D_{LIP\text{-}lat})$

Depending on 5 Model Parameters:
K_{COR}, D_{COR},
K_{LIP}, $D_{LIP\text{-}lat}$, $D_{LIP\text{-}trans}$

How to determine $D_{LIP\text{-}X}$?

- Free energy profiles from MD simulation (Bemporad et al., 2004; Notman & Anwar, 2013)
- Homogenization of Fokker-Planck eqn.

Alternative:

- Experimental data for artificial bilayers, e.g., Xiang,Anderson (1994 ,...),
- Approximation (Nitsche and Kasting, 2013) based on $K_{o/w}$, MW, A, B, S, E ,V

Reconstructed Morphology

w/ E. Sontak, A. Holmes, H. Studier, M. Pastore,
J. Grice, M. Roberts, J. Brandner

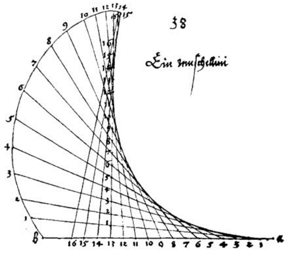

Outlook: From Skin Sample to Simulations

Input: Greyscale TIFF-stack

Output: Geometry for Computation (cell membrane + nuclei)

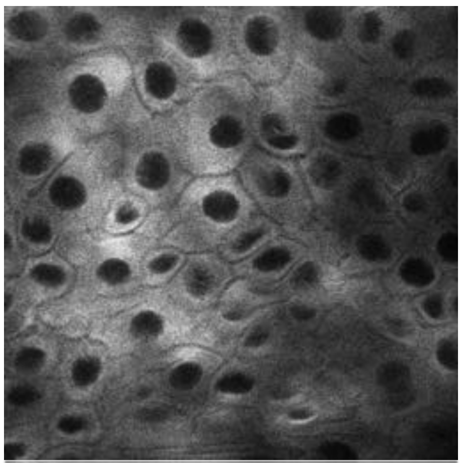

Raw data (H. Studier, A. Holmes, Adelaide)

Steps:

1. Pre-process (anisotropic filter, enhancing light and contrast)
2. Track spherical cell nuclei
3. Membrane reconstruction

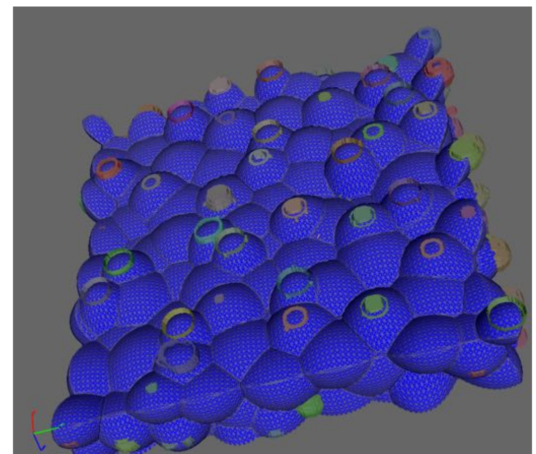

Mesh for Computation (E. Sontak, G-CSC)

Example

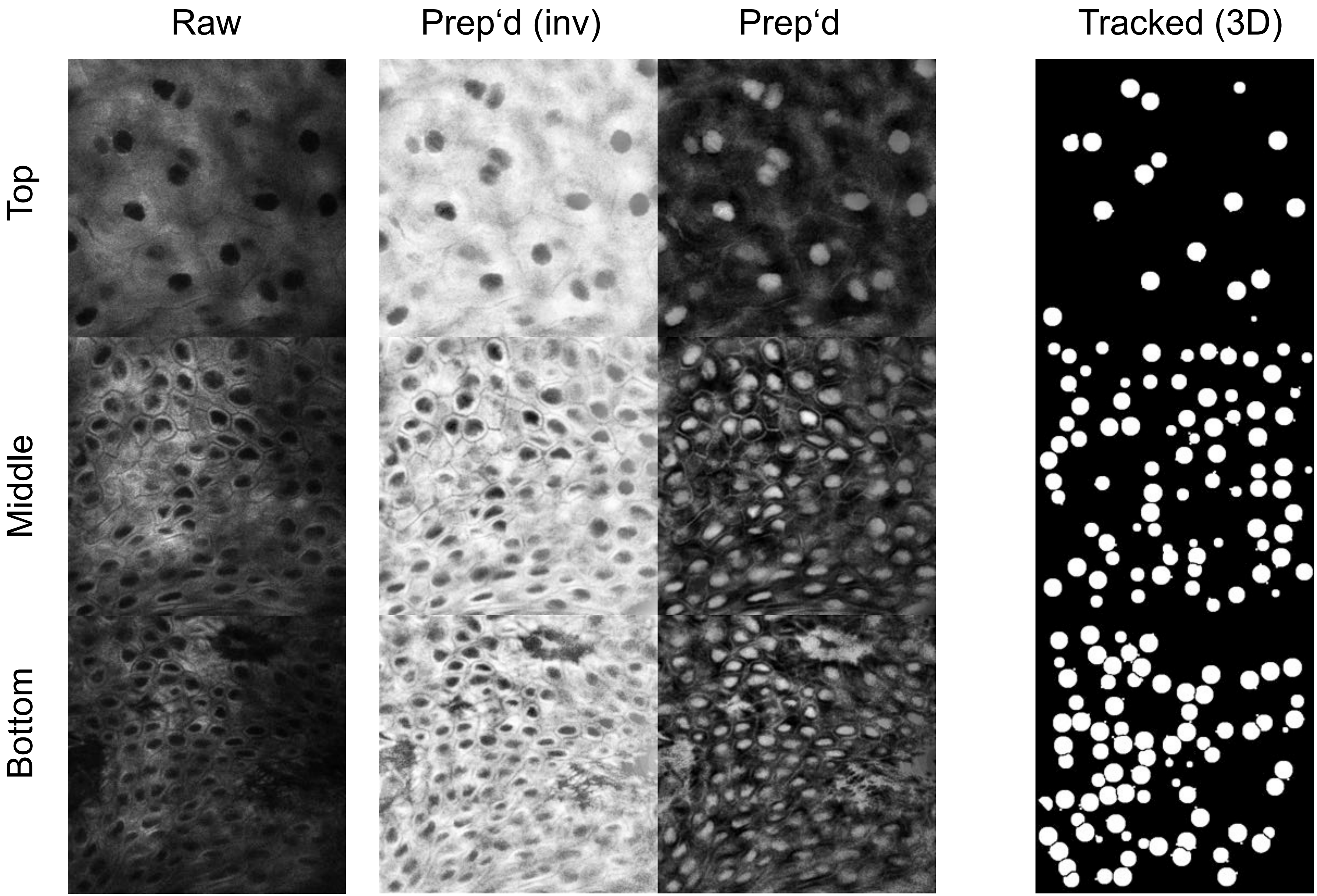

Tracking: Comparison

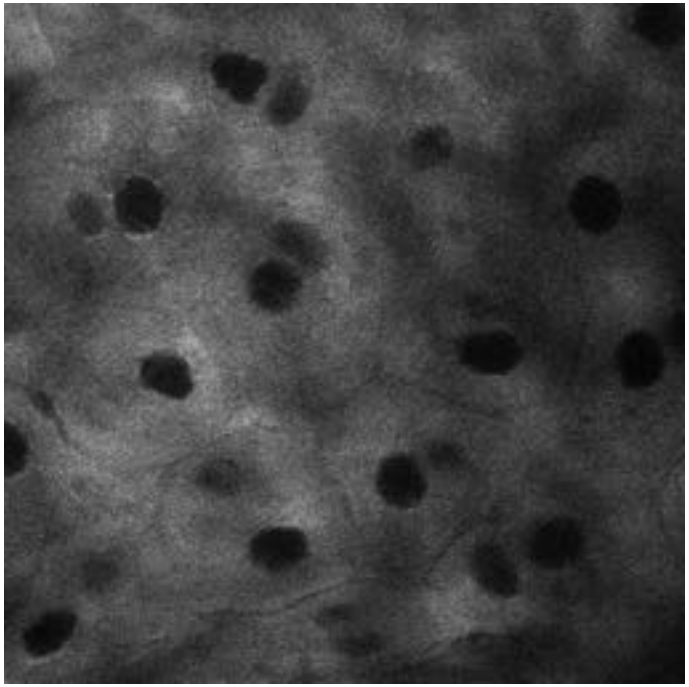

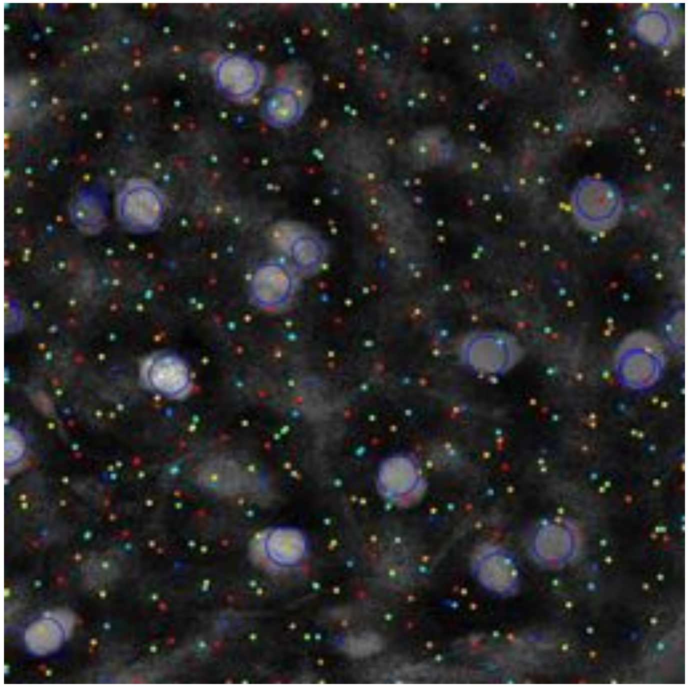

- Sample size: 101 x 101 x 37 um^3
- Found ~600 nuclei (incl. some duplicates and false-positives)
- Nuclei represented as ellipsoids (with different principal axes)
- Large circle → center
- z position color-coded

Preliminary analysis

SGranulosum SSpinosum SBasale

 # Objects/ 100^2 um^2

Occupied area (%)

Area per object (%)

Diameter (10%/50%/90%)

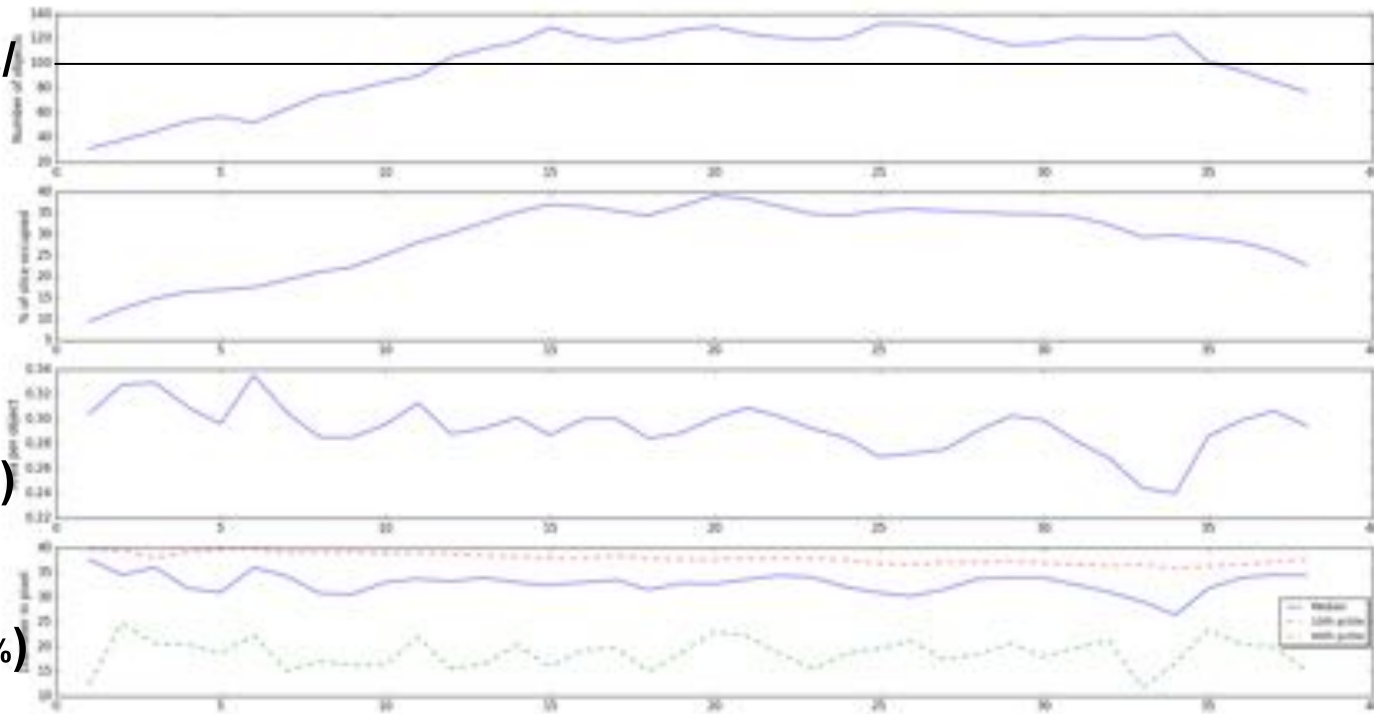

10000 per mm^2

Depth [um]

Reconstructing Cell membranes

For each node p, the **Voronoi region** B(p) is the **set of points** that are **closer to** p **than to any other**.

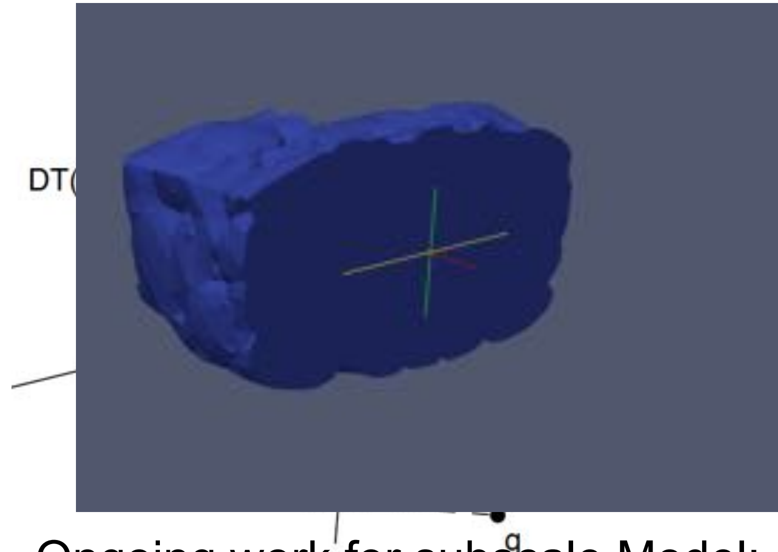

Ongoing work for subscale Model:
Aurenhammer & Klein

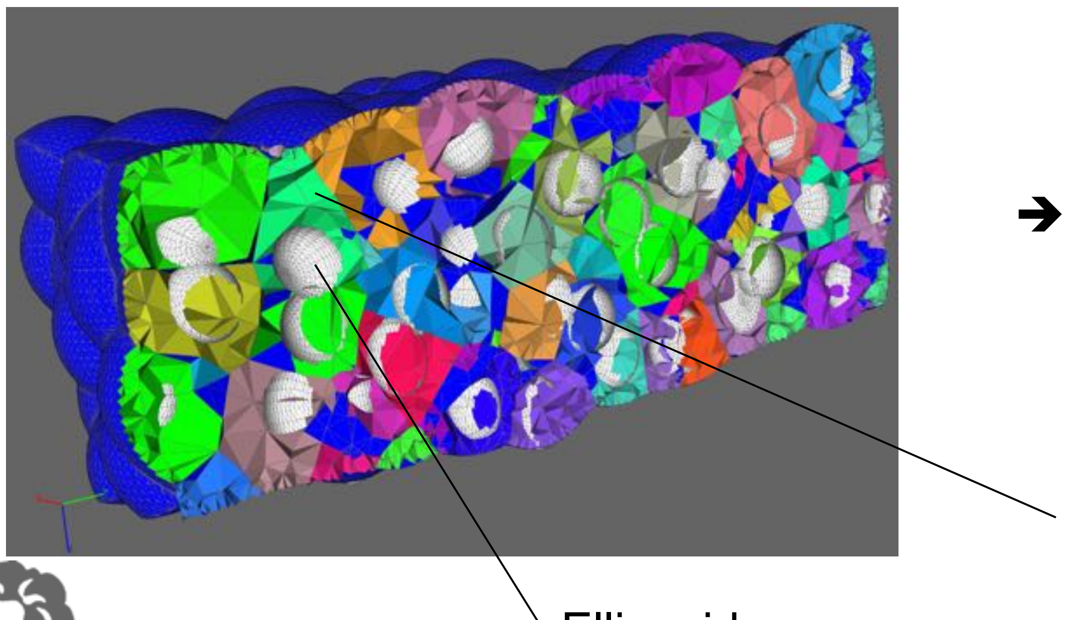

➔ Define cells by Voronoi region $B(c_n)$, where c_n is the center of nucleus n.

A. Nägel, G-CSC, Goethe-University Frankfurt

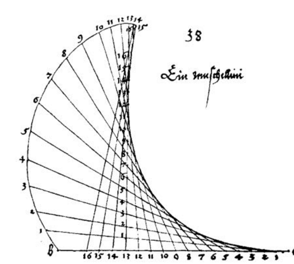

Summary

- The skin is an organ with an inherent **multi-scale structure**;
- **Properties emerge** from the micro-scale to the macro-scale, e.g. influence of cell shape, lipid anisotropy
- Physiology-based bottom-up models provide **accurate infomation** al lower computational complexity
- In-silico tools valuable for **hypothesis testing**
- This allows linking **theoretical findings** with **experiments**
- **Future Perspective:** Merging Simulation and Imaging